Single Crystalline Highly Pure Long Ag2Te Nanowires for Thermoelectric Applications and its Structural Analysis.

Krishnakumar Pillai (krs.pillai21@gmail.com)
Jubail Industrial College https://orcid.org/0000-0002-0988-0054

Research Article

Keywords: Silver telluride, Nanowires, Synthesis, Structure analysis

Posted Date: February 23rd, 2021

DOI: https://doi.org/10.21203/rs.3.rs-220103/v1

Abstract

Ag_2Te is a relatively unexplored promising material, having a variety of potential applications. This paper reports the growth of highly uniform and single crystalline Ag_2Te nanowires by a simple vapor transport method without using a catalyst. The morphology, structure and phase purity of the nanowires were investigated by X-ray diffraction, scanning electron microscopy and transmission electron microscopy. The chemical composition of the individual nanowire was examined by X-ray energy-dispersive spectrometry. Our results revealed the growth of monoclinic Ag_2Te along ($\bar{1}13$) planes. At lower temperatures, hexagonal Te nanowires instead of Ag_2Te nanowires were grown along (001) planes. This strong dependence on the growth temperature suggests a candidate growth mechanism.

1. Introduction

Synthesis of nanostructure materials exhibiting unique properties have become the focus of intensive research due to its potential applications in the fabrication of nanodevices [1–4]. Certain non-magnetic compounds such as silver chalcogenides are promising materials since it exhibits magnetic properties even though their electron spins do not align under external magnetic field. In addition to its interesting giant magneto resistance, silver chalcogenides are attracting widespread interest due to their special semiconducting properties, ionic conductivities and polymorphic phase transitions [5–9]. Especially, silver telluride (Ag_2Te), a relatively unexplored material, has promising applications in low field sensors, optoelectronics, thermoelectric devices and in nanoscale memory devices [10–15]. It exhibits remarkable magneto resistance (MR) at room temperature comparable to the colossal magneto resistance compounds and shows linear field dependence down to 10 Oe. The classical picture seems incapable of explaining the MR of Ag_2Te and the origin is still uncertain though there are some speculating reports [16]. Ag_2Te compound exhibits a first order phase transition at around 418 K. The low temperature phase, monoclinic Ag_2Te referred as hessite, is a semiconductor with a narrow band gap, high carrier mobility and low lattice thermal conductivity, whereas its high temperature phase, cubic, gives rise to super ionic conductivity. An additional silver deficient phase of this compound, referred as empressite ($Ag_{(5-x)}Te_3$), having a hexagonal structure is also argued to exist [17].

Silver tellurides in bulk were synthesized by the solid state reaction at high temperatures, by the reaction of metal-salt solutions in the presence of toxic gas or by the reaction of metal and chalcogen in ammonia, but yielded a mixture of Ag_2Te and 5–10% Ag_7Te_4 [18]. Nanoparticles and nanotubes of crystalline Ag_2Te were also synthesized by high intensity ultrasonic irradiation in organic solvents [19], and by the hydrothermal process [20], respectively. In addition to nanoparticles and nanotubes, nanowires are also unique in their properties relative to the bulk due to the confinement effects and surface effects. Earlier, using electro deposition in anodic alumina membranes and hydrothermal techniques, Ag_2Te nanowire (NW) bundles were synthesized [21], but the NWs were not single-crystalline with a preferred growth orientation. Different morphologies of Ag_2Te nanostructures and nanowires were synthesized by a hydrothermal method [10, 22]. Chang et al, prepared Ag_2Te nanowires by one-step solvothermal method

without templates and surfactants [23]. They also proposed a possible growth mechanism. Growth of high-purity, high-performance nanowires is of considerable technological importance due to many of its unique applications. This paper report the growth of highly crystalline uniform Ag_2Te NWs by a simple vapor transport technique without using a catalyst. As no catalysts are used for the synthesis, the NWs are highly pure.

2. Experimental Section

A typical horizontal two-zone temperature furnace with a 1 inch diameter quartz tube, as shown by a layout in Scheme 1, was used to grow Ag_2Te NWs. The setup is equipped with pressure and mass flow controllers. In order to remove any impurities and to maintain an inert atmosphere, the furnace was evacuated to less than 100 mTorr and then purged with Ar gas for 30 minutes. The precursor, Ag_2Te powder (0.04 g, 99.999%, Sigma-Aldrich) placed in an alumina boat, was evaporated at a temperature of around 1000°C in the upstream zone of the furnace maintaining a pressure at 10 Torr. The vapors carried over by 500 sccm Ar carrier gas were deposited on to Si substrates placed at a distance d (Scheme 1) from the alumina boat kept at the junction between downstream and upstream. The experiment was performed for 30 minutes, keeping a steady flow rate and pressure. The downstream was not heated during the course of the experiment. After the completion of the experiment the furnace was allowed to cool down to room temperature. The NWs that had grown on the substrate were analyzed by X-ray diffraction (XRD), scanning electron microscopy (SEM), transmission electron microscopy (TEM) and energy dispersive X-ray spectroscopy (EDS). The crystal structure of the precursor powder and the final product on the substrate were examined by XRD using Cu Kα radiation (λ = 1.5418 Å). The morphology, structure and phase purity of the NWs were investigated by SEM and TEM. The TEM images, high-resolution TEM (HRTEM) images, and selected area electron diffraction (SAED) patterns were obtained on a JEOL JEM-2100F TEM operated at 200 kV. Chemical composition of the individual NW was examined by X-ray energy-dispersive spectrometry (EDS) attached to the TEM. The samples for TEM analysis were prepared either by dispersing the NWs in solvent followed by placing a drop of the solution on a carbon coated copper grid or by dragging the grids along the surface of the sample.

3. Results And Discussion

Ag_2Te nanowires were grown on Si (111) substrates placed at the junction between upstream and downstream zones using a characteristic two-zone temperature furnace with an inner quartz tube (a layout in Scheme 1). The precursor, kept in an alumina boat and placed at the centre of the upstream zone, was evaporated at 1000°C with a heating rate of 50°C/minute. Figure 1(a) shows the morphology of the NWs as examined by SEM using a Philips XL30SFEG. The high magnified SEM image of a typical single NW (inset of Fig. 1(a)) and the TEM image (Fig. 1(c)) demonstrate that the NWs are clean and highly uniform. The NWs were of 10 to 15 micrometers long and 50 to 250 nm diameter. The XRD pattern of the as-grown NW ensemble (Fig. 1(b)) shows the Bragg diffraction peaks, which were indexed to the monoclinic Ag_2Te structure (JCPDS file: 65-1104), denoting the growth of monoclinic Ag_2Te NWs. The

XRD spectrum did not exhibit any significant characteristic Bragg peak of Ag or Te metal, which excludes significant Ag/Te phase segregation and formation of Ag/Te metal clusters/precipitates in the Ag_2Te nanowires. The TEM image from a representative NW with a diameter of 60 nm is shown in Fig. 1(c). The inset of the figure depicts the selected area electron diffraction (SAED) patterns of the NW. It shows a regular spot pattern, revealing the single-crystalline phase of the NW. The diffraction spots pattern were indexed to monoclinic Ag_2Te structure (JCPDS file: 65-1104), in accordance with XRD pattern of NW ensemble. The NW growth direction was along ($\bar{1}$13) plane. The lattice spacing (d) of 3.96 Å and 4.13 Å were identified as (011) and ($\bar{1}$02) planes respectively, of monoclinic Ag_2Te. Figure 1(d) depicts a HRTEM image and the clear lattice fringes confirm the single crystalline nature of the NWs. The interplanar spacing (d) perpendicular to the growth direction was estimated as 2.34 Å fitting well with the interplanar distance of the ($\bar{1}$13) plane, endorsing the ($\bar{1}$13) growth direction of the NWs in agreement with the SAED findings. The observed interplanar spacing is in concurrence with d = 2.31 Å of ($\bar{1}$13) planes in bulk monoclinic Ag_2Te.

Figure 2 depicts the EDS composition line profile measured across the diameter of the NW and the corresponding spectrum from a single Ag_2Te NW. The spectrum in Fig. 2(c) illustrates that the NW consists of Ag and Te elements. The quantitative analysis indicates that the atomic ratio of Ag to Te is close to 2:1, confirming the growth of Ag_2Te NWs (lines due to Cu is from the TEM grid). The composition line profile measured along the diameter of the NW (Fig. 2(b)) shows a uniform composition of Ag and Te along the cross-section of the NW.

It is noticed that Te NWs were grown on the Si substrate if the experiment was performed at an upstream temperature of 900°C or less, indicating temperature dependence on the growth of NWs. Figure 3(a) shows the morphology of nanowires as examined by SEM. The magnified image in the inset illustrates that the NWs are clean and highly uniform. The XRD pattern (Fig. 3(b)) of the as-grown Te NW ensemble on the Si substrate shows Bragg diffraction peaks that were indexed to hexagonal Te structure (JCPDS file: 36-1452). Figure 3(c) depicts the TEM image of a typical Te NW. The upper inset in the figure depicts the SAED patterns of the NW which shows a regular spot pattern, reflecting the single-crystalline nature of the NW. The diffraction spots pattern were indexed to hexagonal Te structure (JCPDS file: 36-1452), in agreement with XRD pattern of NW ensemble. The NW growth direction was along (001) plane. The lattice spacing (d) of 2.1 Å was identified as (111) plane. Figure 3(d) depicts the high resolution (HR) TEM and the clear lattice fringes indicate that the NW is single crystalline in nature. The interplanar spacing (d) perpendicular to the growth direction was estimated as 5.92 Å fitting well with the interplanar distance of the (001) plane, confirming the (001) growth direction of the NWs. The relevant Fast Fourier transformation pattern is shown in the inset of Fig. 3(d). The EDS spectrum obtained from the marked portion on panel ‘c’ is shown in the lower inset of Fig. 3(c), which confirm that the NW consists of only Te element (lines due to Cu is from the TEM grid).

To deduce a possible NW growth mechanism systematic experiments were carried out at various upstream temperatures and flow rates. Subsequently, EDS analysis was performed at each stage to

determine the type of NWs (i.e. whether the grown NWs are Te, Ag or Ag_2Te). It is found that Te, Ag_2Te or a mixture of Te and Ag_2Te NWs were grown on the substrate, depending on the upstream temperature whereas the flow rate has negligible effect. Further, EDS analysis was also carried out at several spots on the same substrate deposited at each upstream temperature to determine the type of NWs formed. It is observed that the percentage of Ag_2Te NWs increases with temperature whereas that of Te NWs shows the opposite trend. For example, Te NWs were grown for an upstream temperature equal to 900°C or less. In contrast only Ag_2Te NWs dominate in the temperature range 1000–1050°C. In the intermediate temperature at 950°C, EDS analysis indicated the presence of both Te and Ag_2Te compound on the substrate.

This strong dependence of the Te and Ag_2Te NWs percentage on the temperature can be explained in the following way. Ag_2Te compound is known to start to dissociate even at temperatures as low as 750°C, depositing mostly Te on the substrate at low temperature [24]. This is because the evaporation rate of Te atoms is greater than those of Ag atoms and Ag_2Te molecules. The strong reactivity of Ag and Te ($(G_{Ag2Te})_{298}$ = -81.66 kJ mol^{-1}) is also known [25]. Thus during the heating of Ag_2Te powder in the upstream, the precursor dissociates and the vapors of Ag and Te carried over to the downstream of the apparatus by the Ar carrier gas recombine on the Si substrate to form Ag_2Te nuclei, which may act as seeds facilitating the growth of Ag_2Te NWs. The nucleation of Ag_2Te from Ag and Te elements requires diffusion of the two species. It is also well known that the diffusivity of Ag in Te (4×10^5 $Å^2$/s at 300 K) is larger than that of Te in Ag (2.429×10^{-12} $Å^2$/s at 300 K) [26]. Therefore the structure and phase formation of the material grown on the substrate must be dictated mostly by the diffusion of Ag in Te lattice. The sequential growth of Ag_2Te nanocrystals by diffusion and the phase formation was earlier studied by high resolution transmission electron microscopy [27].

When the experiment is performed at low temperatures, transportation of Te after dissociation of the precursor is favored and hence the growth of Te NWs dominates at temperatures ≤ 900°C. As the temperature increase, the evaporation rates of both Te and Ag increases so that a mixture Te and Ag_2Te was obtained on the Si substrate. The vapor pressure data for pure Ag and Te suggests that vapor pressure of silver increases faster with temperature than that of tellurium [24]. Hence it seems that at our experimental condition of 1000–1050°C, after the deposition of Ag and Te atoms on the substrate, Ag_2Te NWs have grown by self-seeded process through diffusion and reaction.

4. Conclusion

In conclusion, this report demonstrated the growth of highly uniform and single crystalline Ag_2Te and Te NWs by a simple vapor transport method without using a catalyst. The morphology, structure and phase purity of the NWs were investigated by XRD, SEM and TEM. The HRTEM and SAED analysis revealed the growth of monoclinic Ag_2Te and hexagonal Te NWs along $(\bar{1}13)$ and (001) planes, respectively. The possible NW growth mechanism is deduced from various experiments carried out at different growth

conditions. It is expected that these NWs could be used for studies of transport properties and magneto resistance behavior. Further, this simple approach will provide growth of Ag_2Te NWs and related silver chalcogenides in a controlled manner for many important applications in nanodevices.

Declarations

Acknowledgement

The author acknowledges the support by the Jubail Industrial College and Royal Commission in Jubail.

References

1. Sahu, B. Russ, M Liu, F Yang, E W. Zaia, M P. Gordon, J D. Forster, Y.Q Zhang, M. C. Scott, K A. Persson, N E. Coates, R A. Segalman, J J. Urban, Nat. Commun. 11(2020), p. 2069
2. E Pomerantseva, F Bonaccorso, X Feng, Y Cui, Y Gogotsi, Science, 366 (2019), p. 6468
3. X Pan, X Hong, L Xu, Y Li, M Yan and L Mai, Nano Today, 28 (2019), p. 100764
4. Jos E. M. Haverkort, Erik C. Garnett, and Erik P. A. M. Bakkers, Appl. Phys. Rev., 5 (2018), 031106
5. Xu, A. Husmann, T. F. Rosenbaum, M.-L. Saboungi, J. E. Enderby, P. B. Littlewood, Nature, 390 (**1997)**, 57.
6. Hu, T. F. Rosenbaum, J. B. Betts, Phys. Rev. Lett. 95 (2005), 186603.
7. Q. Liang, X. Chen, Y. J. Wang, Y. J. Tang, Phys. Rev. B 61 (2000), 3239.
8. Chen, D. S. Xu, G. L. Guo, L. I. Gui, Electrochimica Acta, 49 (2004), 2243.
9. Chen, D. S. Xu, G. L. Guo, Y.Tang, Chem. Phys. Lett. 377 (2003), 205.
10. Gao, K. Wang, H. Song, H.Wu, S.Yan, X. Xu, Y.Shi, J. Nanosci. Nanotechnol., 20 (2020), 2628.
11. Kumar, S. Rani, Y. Singh, V. N. Singh, J. Nanosci. Nanotechnol., 20 (2020), 3636.
12. K Premasiri, W Zheng, B Xu, T Ma, L Zhou, Y Wu, X P. A. Gao, Nanoscale, ,11 (2019),
13. X Zeng, L Ren, J Xie, D Mao, M Wang, X Zeng, G Du, R Sun, J-B Xu, C-P Wong, ACS Appl. Mater. Interfaces, 11(41) (2019), 37892.
14. X Zeng C Yan L Ren T Zhang F Zhou X Liang N Wang R Sun J-B Xu C-P Wong, Adv. Electron. Mater. 5 (2019), 1800612.
15. H Yang, J-H Bahk, T Day, A M. S. Mohammed, B Min, G. J Snyder, A Shakouri, Y Wu, Nano Lett., 14 (2014),
16. Xiong, S.-D. Wang, X. R. Wang, Phys. Rev. B,*61* (2000), 14335.
17. Donnay, F. C. Kracek, W. R. Jr. Rowland, Am. Mineralogist,41 (1956), 1956.
18. Henshaw, I. P. Parkin, G. Shaw, Chem. Commun., 21 (1996), 1095; C. J. Warren, R. C. Haushalter, A. B. Bocarsly, J. Alloys Compound,229(1995), 175.
19. Li, Y. Xie, Y. Liu, J. X. Huang, Y. T. Qian, J. Solid State Chem. 158 (2001), 260.

20. M. Qin, Y. P. Fang, P. Tao, J. Zhang, C. Y. Su, Inorg. Chem. 46 (2007), 7403.
21. Chen, D. S. Xu, G. Guo, L. Gui, J. Mater Chem. 12 (2002), 2435; L. Zhang, J. C. Yu, M. Mo, L. Wu, K. W. Kwong, Q. Li, Small,1 (2005), 349.
22. Gholamrezaei, M S Niasari, D Ghanbari, B. Samira, Sci. Rep. 6 (2016), 20060.
23. Y Chang , J Guo , Y-Q Tang , Y-X Zhang , J Feng, Z-H Ge, CrystEngComm, 21 (2019), 1718.
24. Dalven, J. Appl. Phys. 37 (1966), 2271.
25. C. Millis, Thermodynamic Data for Inorganic Sulphides, Selenides and Tellurides, Butterworth, London, **1974.**
26. J. Hauser, in Proc. 9^{th} Int. Conf. On Cryst. And Amor. Semicond., Grenoble, France, J. de. Phys. (Paris) 42 (1981), C4-943.
27. Hirota, T. Isshiki, K. Okashita, M. Shiojiri, J. Cryst. Growth,112 (1991), 55.

Figures

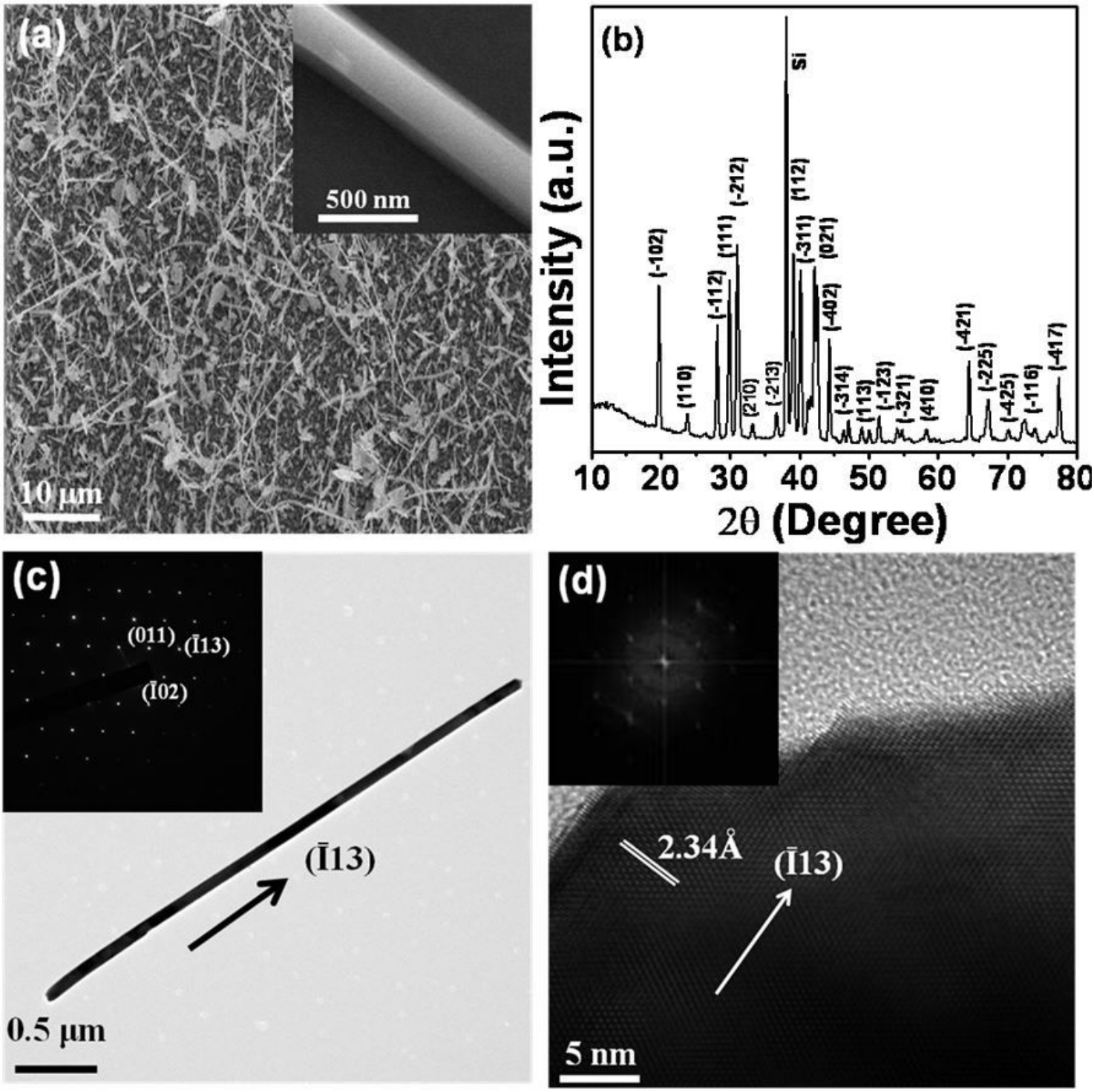

Figure 1

(a) Representative SEM image of Ag2Te nanowires grown by vapor transport method on Si (100) substrate at an upstream temperature of 1000 ºC. The inset represents high magnification SEM image of a typical nanowire. (b) XRD Pattern of the as-grown Ag2Te nanowire ensemble on Si substrate at an upstream temperature of 1000 ºC. The Bragg diffraction peaks were indexed to monoclinic Ag2Te (JCPDS file: 65-1104). (c) Representative TEM image of Ag2Te nanowire grown along (Ī13) plane. The arrow mark indicates the growth direction of nanowire. Inset shows SAED pattern, indexed to monoclinic

Ag2Te structure. The lattice spacing of 3.96 Å and 4.13 Å were identified as the interplanar distances of (011) and ($\bar{1}$02) planes, respectively. (d) Representative HRTEM image of the nanowire shown in panel (c). The lattice spacing 2.34 Å corresponds to the interplanar distance of ($\bar{1}$13) plane. Inset in the figure shows the two dimensional Fast Fourier transform.

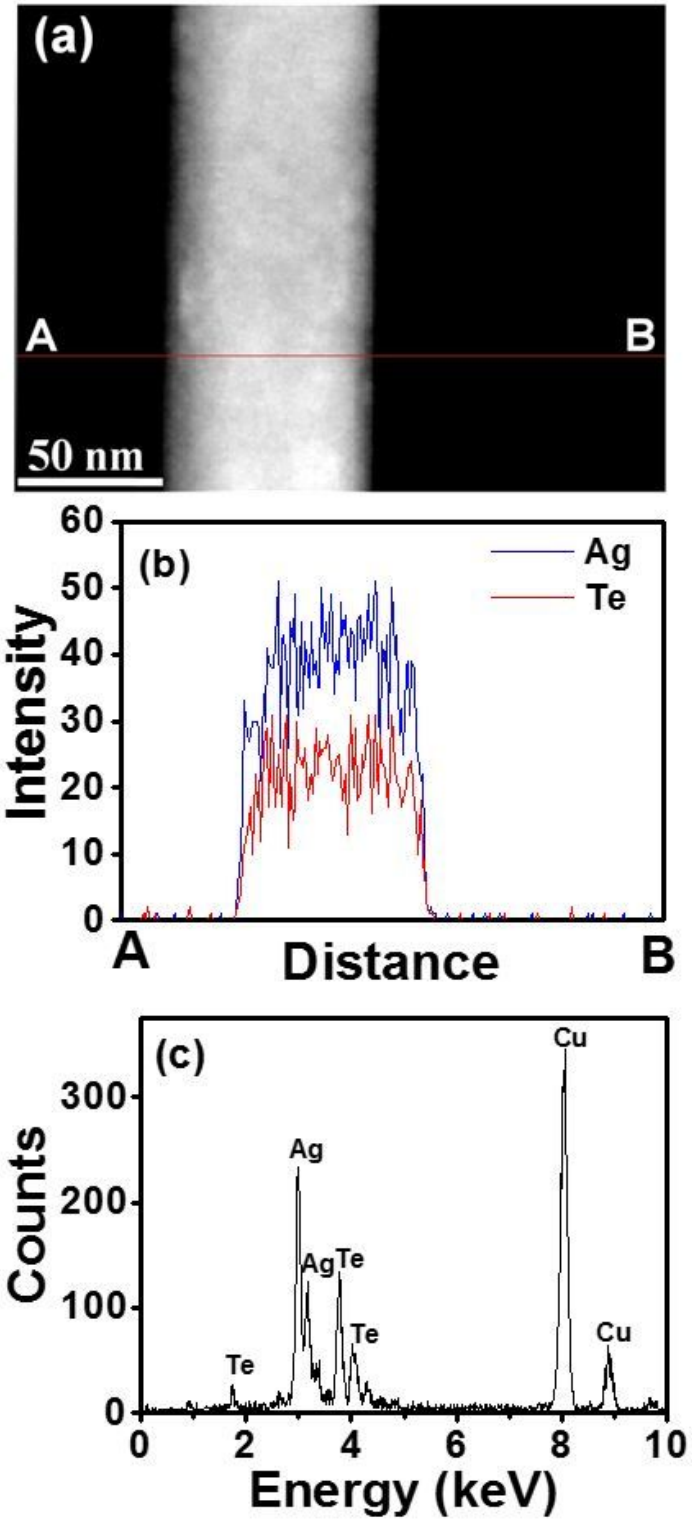

Figure 2

EDS composition line profile analysis along the diameter of a typical Ag2Te nanowire. (a) TEM image of a typical nanowire (white region) and the scan direction is along the marked line AB. (b) EDS compositional (Ag and Te) line profiles along the diameter of the nanowire from A to B as shown in panel (a). (c) EDS spectrum illustrating the composition elements in the nanowire (lines due to Cu is from the TEM grid).

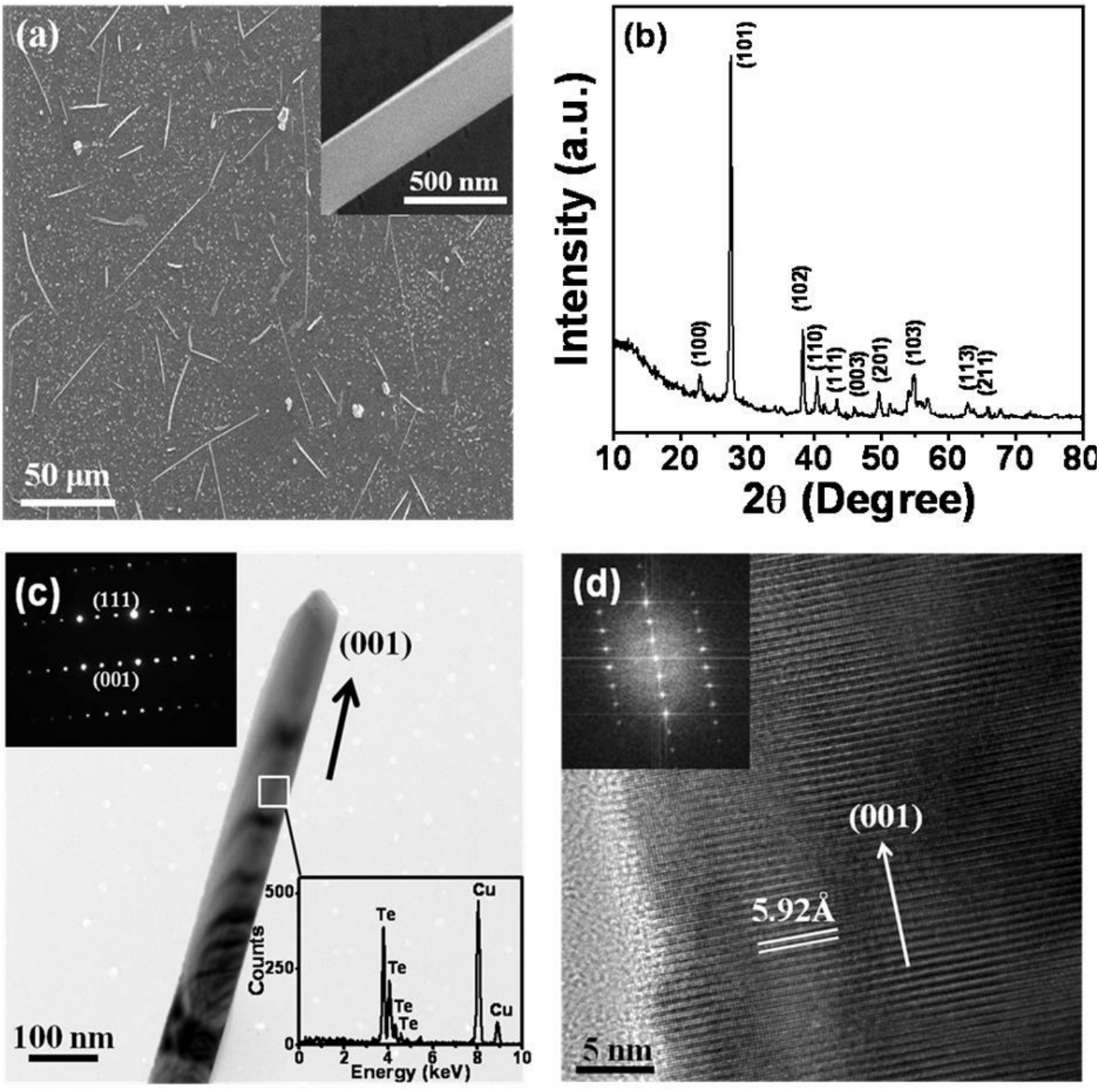

Figure 3

(a) Representative SEM image of Te nanowires grown on Si (100) substrate at an upstream temperature of 900 ºC. The inset represents high magnification SEM image of a typical nanowire. (b) XRD Pattern of the as-grown Te nanowire ensemble on Si substrate at an upstream temperature of 900 ºC. The Bragg diffraction peaks were indexed to hexagonal Te (JCPDS File No: 36-1452). (c) Representative TEM image of a nanowire grown along (001) plane. The arrow mark indicates the growth direction of nanowire. Upper inset shows SAED pattern, indexed to hexagonal Te structure. The lattice spacing of 2.1 Å was identified as (111) plane. Lower inset shows EDS spectrum of nanowire examined from the marked portion in panel (lines due to Cu is from the TEM grid). (d) Representative HRTEM image of the nanowire shown in panel (c). The lattice spacing 5.92 Å corresponds to the interplanar distance of (001) plane. Inset in the figure shows the two dimensional Fast Fourier transform.

Supplementary Files

This is a list of supplementary files associated with this preprint. Click to download.

- scheme1.jpg